



Heterogeneity of EEG resting-state brain networks in absolute pitch

Greber, Marielle ; Klein, Carina ; Leipold, Simon ; Sele, Silvano ; Jäncke, Lutz

Abstract: The neural basis of absolute pitch (AP), the ability to effortlessly identify a musical tone without an external reference, is poorly understood. One of the key questions is whether perceptual or cognitive processes underlie the phenomenon as both sensory and higher-order brain regions have been associated with AP. To integrate the perceptual and cognitive views on AP, here, we investigated joint contributions of sensory and higher-order brain regions to AP resting-state networks. We performed a comprehensive functional network analysis of source-level EEG in a large sample of AP musicians ($n = 54$) and non-AP musicians ($n = 51$), adopting two analysis approaches: First, we applied an ROI-based analysis to examine the connectivity between the auditory cortex and the dorsolateral prefrontal cortex (DLPFC) using several established functional connectivity measures. This analysis is a replication of a previous study which reported increased connectivity between these two regions in AP musicians. Second, we performed a whole-brain network-based analysis on the same functional connectivity measures to gain a more complete picture of the brain regions involved in a possibly large-scale network supporting AP ability. In our sample, the ROI-based analysis did not provide evidence for an AP-specific connectivity increase between the auditory cortex and the DLPFC. The whole-brain analysis revealed three networks with increased connectivity in AP musicians comprising nodes in frontal, temporal, subcortical, and occipital areas. Commonalities of the networks were found in both sensory and higher-order brain regions of the perisylvian area. Further research will be needed to confirm these exploratory results.

DOI: <https://doi.org/10.1016/j.ijpsycho.2020.07.007>

Posted at the Zurich Open Repository and Archive, University of Zurich

ZORA URL: <https://doi.org/10.5167/uzh-189036>

Journal Article

Published Version



The following work is licensed under a Creative Commons: Attribution 4.0 International (CC BY 4.0) License.

Originally published at:

Greber, Marielle; Klein, Carina; Leipold, Simon; Sele, Silvano; Jäncke, Lutz (2020). Heterogeneity of EEG resting-state brain networks in absolute pitch. *International Journal of Psychophysiology*, 157:11-22.

DOI: <https://doi.org/10.1016/j.ijpsycho.2020.07.007>



Heterogeneity of EEG resting-state brain networks in absolute pitch

Marielle Greber^{a,*}, Carina Klein^a, Simon Leipold^{a,b}, Silvano Sele^{a,c}, Lutz Jäncke^{a,c,*}

^a Division Neuropsychology, Department of Psychology, University of Zurich, Zurich, Switzerland

^b Department of Psychiatry and Behavioral Sciences, Stanford University School of Medicine, Stanford, USA

^c University Research Priority Program (URPP), Dynamics of Healthy Aging, University of Zurich, Zurich, Switzerland



ARTICLE INFO

Keywords:

Musicians
Absolute pitch
EEG
Replication
Functional connectivity
Resting state

ABSTRACT

The neural basis of absolute pitch (AP), the ability to effortlessly identify a musical tone without an external reference, is poorly understood. One of the key questions is whether perceptual or cognitive processes underlie the phenomenon, as both sensory and higher-order brain regions have been associated with AP. To integrate the perceptual and cognitive views on AP, here, we investigated joint contributions of sensory and higher-order brain regions to AP resting-state networks.

We performed a comprehensive functional network analysis of source-level EEG in a large sample of AP musicians ($n = 54$) and non-AP musicians ($n = 51$), adopting two analysis approaches: First, we applied an ROI-based analysis to examine the connectivity between the auditory cortex and the dorsolateral prefrontal cortex (DLPFC) using several established functional connectivity measures. This analysis is a replication of a previous study which reported increased connectivity between these two regions in AP musicians. Second, we performed a whole-brain network-based analysis on the same functional connectivity measures to gain a more complete picture of the brain regions involved in a possibly large-scale network supporting AP ability.

In our sample, the ROI-based analysis did not provide evidence for an AP-specific connectivity increase between the auditory cortex and the DLPFC. The whole-brain analysis revealed three networks with increased connectivity in AP musicians comprising nodes in frontal, temporal, subcortical, and occipital areas. Commonalities of the networks were found in both sensory and higher-order brain regions of the perisylvian area. Further research will be needed to confirm these exploratory results.

1. Introduction

Absolute pitch (AP) is the rare ability to effortlessly identify the pitch of a musical tone without the aid of an external reference tone (Deutsch, 2013). The neural mechanisms underlying AP are poorly understood. One central issue concerns the question of to what extent perceptual and cognitive processes contribute to the phenomenon. On the one hand, evidence from both structural and functional neuroimaging points towards an involvement of auditory regions (Keenan et al., 2001; McKetton et al., 2019; Schlaug et al., 1995), supporting the view of altered perceptual processing in AP (Kim and Knösche, 2017a). On the other hand, the two-component model, a prominent cognitive theory of AP, postulates that the association of long-term pitch representations with their labels (pitch labeling) constitutes the neurophysiological fundament of AP (Levitin, 1994). This pitch-labeling process has been associated with neural activation in the dorsolateral prefrontal cortex (DLPFC) (Bermudez and Zatorre, 2005; Zatorre et al., 1998).

Aiming to integrate the perceptual and cognitive perspectives on AP, the current study examined EEG resting-state connectivity for contributions of both sensory and higher-order brain regions to AP networks. Electroencephalographic resting-state activity has repeatedly been demonstrated to contain stable individual-specific information (e.g., Näpflin et al., 2007; Paranjape et al., 2001; Poulos et al., 2002; Valizadeh et al., 2019). Additionally, it has been shown that music-specific networks can be observed during resting state: Professional musicians exhibit increased EEG resting-state connectivity between brain regions that are involved in music processing and music production (Klein et al., 2015). Resting-state connectivity patterns in AP musicians might similarly reflect a network of brain regions underlying this specific expertise.

Analyzing resting-state EEG, a previous study of our group (Elmer et al., 2015) found some evidence that the auditory cortex and the DLPFC in the left hemisphere were functionally more strongly connected in AP musicians than in non-AP musicians. However, the study focused solely on these two regions of interest (ROIs) within each

* Corresponding authors at: Binzmühlestrasse 14, Box 25, CH-8050 Zürich, Switzerland.

E-mail addresses: marielle.greber@uzh.ch (M. Greber), lutz.jaencke@uzh.ch (L. Jäncke).

<https://doi.org/10.1016/j.ijpsycho.2020.07.007>

Received 27 April 2020; Received in revised form 9 July 2020; Accepted 19 July 2020

Available online 25 July 2020

0167-8760/ © 2020 The Authors. Published by Elsevier B.V. This is an open access article under the CC BY license (<http://creativecommons.org/licenses/by/4.0/>).

hemisphere. While this ROI-based approach minimizes the multiple comparisons problem, it neglects the possibility that the two ROIs could be part of a more extensive network. According to current scientific knowledge, various cognitive functions rely on interactions between distributed brain regions organized within large-scale networks (Bressler and Menon, 2010; Fuster, 2006; Petersen and Sporns, 2015; Sporns et al., 2004). The same might apply to AP. Findings from fMRI resting-state studies are in line with a more widespread resting-state network in AP musicians. A graph-theoretical study revealed increased clustering, degrees, strength, and local efficiency during rest in AP musicians not only in the superior temporal gyrus but also on a whole-brain level (Loui et al., 2012). Another fMRI study reported increased resting-state connectivity between the right planum polare and the auditory cortex (Kim and Knösche, 2017b). More recently, Brauchli et al. (2019a) identified increased local resting-state functional connectivity in the left anterior middle frontal gyrus (in the vicinity of the DLPFC) and in the left intraparietal sulcus, and increased global resting-state functional connectivity in the right superior parietal lobule. This suggests an AP-specific network in higher-order cognitive areas. However, when applying multivariate pattern analysis (MVPA), which can capture more fine-grained connectivity patterns, the classification accuracy for AP and non-AP musicians was highest in the left Heschl's gyrus.

Taken together, AP-specific resting-state networks may rely on additional temporo-frontal connections besides the one between the auditory cortex and the DLPFC. Whole-brain analyses provide an opportunity to explore this potential involvement of other regions in an AP-specific network. On the downside, in case of stringent multiple testing correction, whole-brain analyses may miss regional connectivity differences that could have been picked up by ROI-based analyses.

A common limitation of most previous neuroscientific studies comparing AP and non-AP musicians are small sample sizes. This is mostly due to the low prevalence of AP as well as the resource-intensive data acquisition in neuroimaging. Small samples result in low statistical power and unreliable estimates of the true effect (Button et al., 2013). Therefore, studies with larger samples are urgently needed to advance our understanding of the neural underpinnings of AP.

Using a large sample of musicians with AP ($n = 54$) and without AP ($n = 51$), we here reevaluate the question of whether AP musicians demonstrate specific functional resting-state connectivity patterns. We recorded resting-state EEG and employed well-established source estimation techniques to measure functional connectivity. For AP research, EEG-based measures might be particularly suited to estimate neurophysiological coactivations during rest since, in contrast to resting-state fMRI recordings, the data is acquired in silence without background noise. The current study further benefits from the application of several connectivity measures (lagged phase synchronization, lagged linear connectivity, and instantaneous linear connectivity), which are each associated with different strengths and weaknesses regarding volume conduction, individual-specific stability, and relation to structural connectivity as described in detail below (see section on 'EEG Source-Level Connectivity' in 'Material and Methods').

To combine the methodological advantages of both ROI-based and whole-brain analyses, we adopted two approaches: (1) We conducted an ROI-based analysis to examine the functional connectivity between the auditory cortex and the DLPFC. This part of the study is a replication of the above-described previous study of our group (Elmer et al., 2015), which had a much smaller sample. (2) We conducted a whole-brain connectivity analysis to explore a potential involvement of other regions besides the auditory cortex and the DLPFC with regard to a more widespread AP-specific network. This analysis was guided by the findings discussed above, which suggest distributed network features in AP musicians comprising brain areas other than the auditory cortex and the DLPFC.

2. Materials and methods

2.1. Participants

Fifty-four AP musicians and 51 non-AP musicians aged 18–44 years participated in the EEG resting-state study. All participants were professional musicians, music students, or highly-trained amateur musicians, who were recruited within a larger research project investigating the neural correlates of AP (Brauchli et al., 2019a, 2019b; Burkhardt et al., 2019, 2020; Greber et al., 2018; Leipold et al., 2019a, 2019c, 2019d). The participants were assigned to the two groups based on self-report. Before being invited to the study, participants underwent online testing assessing demographic information, musical experience, and pitch-labeling ability. Based on these data, the two groups were matched for sex, age, handedness, age of onset of musical training, and cumulative hours of musical training over the lifespan.

None of the participants reported any audiological, neurological, or severe psychiatric disorders. Pure-tone audiometry (MAICO ST 20, MAICO Diagnostic, GmBh, Berlin) confirmed normal hearing thresholds in all participants. Self-reported handedness was validated using a German translation of the Annett Handedness Questionnaire (Annett, 1970). To ensure group comparability with regard to general cognitive abilities, intelligence was evaluated using the Mehrfachwahl-Wortschatz-Intelligenztest (MWT-B; Lehrl, 2005). Musical aptitude was estimated using the Advanced Measures of Music Audiation (AMMA; Gordon, 1989). The AMMA consists of 30 pairs of piano melodies. Participants are asked to decide whether the two melodies are identical, different in rhythmical patterns, or different in tonal patterns. The test results in a rhythmical score, a tonal score, and a total score (which equals the sum of rhythmical and tonal score). Characteristics of the two groups are given in Table 1, the results of the statistical comparisons are provided in the Results section (see section 'Statistical Analyses of Demographic and Behavioral Data').

The study was approved by the ethics committee of the canton of Zurich (<http://www.kek.zh.ch>) and was performed in accordance with

Table 1
Participant characteristics.

	Absolute Pitch Musicians ($n = 54$)		Non-Absolute Pitch Musicians ($n = 51$)	
Sex				
Female	27		24	
Male	27		27	
Age (years)	26.67	(5.49)	25.37	(4.49)
Handedness				
Right-handed	47		46	
Left-handed	4		4	
Both-handed	3		1	
Intelligence (MWT-B) ^a	27.69	(5.10)	29.10	(4.64)
Age of Onset of Musical Training (years)	5.93	(2.39)	6.49	(2.44)
Lifetime Cumulative Training (hours) ^b	1.66	(1.22)	1.35	(0.96)
Musical Aptitude (AMMA) ^a – total	66.11	(6.31)	63.35	(6.86)
Musical Aptitude (AMMA) ^a – tonal	32.33	(3.75)	30.45	(4.13)
Musical Aptitude (AMMA) ^a – rhythmical	33.78	(2.83)	32.90	(3.03)
Pitch-labeling Task (%)	76.41	(19.55)	24.04	(18.92)

Annotations. Continuous measures are given as mean (standard deviations in parentheses). Abbreviations: MWT-B = Mehrfachwahl-Wortschatz-Intelligenztest, AMMA = Advanced Measures of Music Audiation. Statistical comparisons for the behavioral and demographic data are listed in the Results section.

^a Raw scores.

^b Units are given in 10,000.

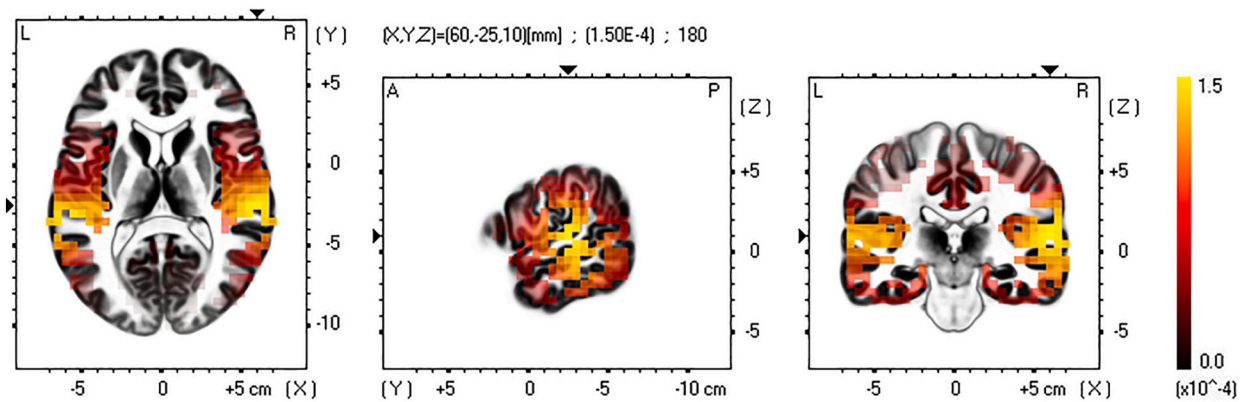


Fig. 1. Validation of the source reconstruction in eLoreta. Current density maps of grand-averaged P1-N1 source activity (80 ms - 170 ms after stimulus onset) evoked by the standard tone C4 ($f_0 = 264$ Hz) in a passive auditory oddball paradigm (Greber et al., 2018) recorded immediately after the resting state. Shown are horizontal, sagittal, and coronal views (from left to right). Source-level activity was maximal in bilateral auditory regions, confirming reasonable source-estimation accuracy in our setup.

the Declaration of Helsinki. Written informed consent was obtained from all participants.

3. Pitch-labeling task

Pitch-labeling ability was evaluated using a web-based adaptation of a task previously applied by our research group (Oechslin et al., 2010b). The task consisted of 108 trials with pure tones ranging from C3 to B5 (tuning: A4 = 440 Hz). In every trial, 2000 ms of Brownian noise, a 500-ms pure tone, and again 2000 ms of Brownian noise were sequentially presented. Overall, each tone appeared three times in a pseudorandomized presentation order: No tone was repeated in successive trials.

Participants were asked to identify the pitch class (chroma, e.g., G) and octave (e.g., 4) of the pure tone by choosing one label (e.g., G4) out of a list of all possible labels (C3 to B5). Trials could be terminated by clicking on a button and had a maximal duration of 15,000 ms. Pitch-labeling accuracy was calculated as the percentage of correctly identified pitch classes. Octave errors were not penalized, resulting in a chance level of 8.3%.

3.1. EEG recording and preprocessing

For EEG recording, participants were seated in an electrically shielded, dimly lit room and instructed to relax with their eyes closed. The eyes-closed resting-state EEG was recorded for three minutes with a sampling rate of 1000 Hz using a BrainAmp amplifier (Brainproducts, Munich, Germany). The 32 silver/silver-chloride electrodes were mounted on an electrode cap (Easycap, Herrsching, Germany) according to a subset of the 10/10 system (Fp1, Fp2, F7, F3, Fz, F4, F8, FT7, FC3, FCz, FC4, FT8, T7, C3, Cz, C4, T8, TP9, TP7, CP3, CPz, CP4, TP8, TP10, P7, P3, Pz, P4, P8, O1, Oz, and O2). An electrode on the tip of the nose served both as an online and offline reference. During EEG acquisition, a bandpass filter of 0.1–100 Hz was applied, and electrode impedances were kept below 10 k Ω by application of an abrasive and electrically conductive gel. After recording of the resting-state EEG, participants performed a passive auditory oddball task (published in Greber et al., 2018) and a pitch-processing task (published in Leipold et al., 2019c, 2019d). In the current study, we only report the resting-state data.

The acquired resting-state EEG data were preprocessed using the BrainVision Analyzer software package (Version 2.1, <https://www.brainproducts.com/>). First, a bandpass filter between 1 and 20 Hz (48 dB/octave), and a notch filter of 50 Hz were applied. Then, a restricted infomax independent component analysis (ICA; Jung et al., 2000) was used to correct eye movement artifacts. Based on visual

inspection, noisy channels were excluded from the ICA and interpolated after ICA correction. Finally, the continuous EEG was divided into segments of 2000 ms. Segments with a voltage gradient > 100 μ V/ms, an amplitude > 200 μ V, or an amplitude < -200 μ V were automatically rejected, resulting in a minimum of 62 and maximum of 90 artifact-free segments per participant. The number of artifact-free segments was comparable between AP and non-AP musicians (mean number of segments for AP musicians = 88.69, mean number of segments for non-AP musicians = 89.67; $t_{(59.71)} = -1.66$, $p = .10$, $d = 0.32$).

3.2. EEG source-level estimation

To compute source-level EEG functional connectivity, the EEG segments were imported into the sLORETA/eLORETA (standardized/exact low-resolution brain electromagnetic tomography) toolbox (Version v20151222, <http://www.uzh.ch/keyinst/loreta.htm>). There, the neural generators of the electric potential differences on the scalp were estimated using the eLORETA algorithm (Pascual-Marqui et al., 2011), a linear, weighted minimum inverse solution with exact localization to point sources. eLORETA uses a realistically shaped head model (Fuchs et al., 2002) based on the Montreal Neurological Institute (MNI) 152 template (Mazziotta et al., 2001) for source reconstruction. The three-dimensional cortical solution space is restricted to gray matter and comprises 6239 voxels with a size of $5 \times 5 \times 5$ mm³. To validate the accuracy of the source reconstruction, we used EEG data from the passive auditory oddball task performed by the same participants immediately after the resting-state recording (Greber et al., 2018). Participants were instructed to focus their attention on a silent movie and to ignore the simultaneously presented piano tones. Based on the grand average over all participants, we estimated the source activity of the P1-N1 complex (80 ms - 170 ms after stimulus onset) of the event-related potential evoked by the standard tone C4 (piano tone with a fundamental frequency $f_0 = 264$ Hz). Current density was maximal in bilateral auditory cortices (see Fig. 1), confirming that the eLORETA algorithm performed as intended on our data.

3.3. EEG source-level connectivity

Based on the estimated source-level activity of the EEG resting-state segments, we conducted two types of connectivity analyses: an ROI-based replication analysis and an exploratory whole-brain network analysis. For both analyses, source-level EEG functional connectivity was evaluated with lagged phase synchronization, lagged linear connectivity, and instantaneous linear connectivity. Lagged phase synchronization is the connectivity measure used in Elmer et al.'s (2015)

study. It quantifies the similarity between the normalized Fourier transforms of two signals (i.e. the time series in one brain region and the time series in another brain region) at a specific frequency after removal of the instantaneous, zero-phase contribution. It is a measure of non-linear dependency, is insensitive to amplitude information, and takes values between zero (independence) and one (perfect similarity). The two additionally analyzed connectivity measures, on the other hand, describe the linear coherence-type similarity between two signals at a specific frequency and incorporate both phase and amplitude information. They are also non-negative but have no upper bound (i.e., infinity corresponds to perfect similarity). Their sum equals the total linear connectivity, whereby the lagged part is only minimally affected by non-physiological artifacts, as for example volume conduction and the low spatial resolution (Pascual-Marqui, 2007; Pascual-Marqui et al., 2011). Contrary to lagged measures, instantaneous measures of connectivity are contaminated with non-physiological artifacts. Yet, they have been shown to surpass lagged measures in biometric identification of individuals (Valizadeh et al., 2019) and in the proportion of variance explained by structural connectivity (Finger et al., 2016). Furthermore, instantaneous connectivity measures have been successfully used to obtain meaningful expertise-related resting-state networks in previous studies (e.g., Jäncke and Langer, 2011; Klein et al., 2015, 2018). Hence, (near) zero-lag dependency seems to carry some relevant physiological information that is not fully captured by lagged measures. For instance, a recent study using intracranial recordings found that inter-hemispheric connectivity between homologous regions is often zero-lagged (preprint: O'Reilly and Elsabbagh, 2020). The use of the described connectivity measures enabled us to examine phase-only and phase-amplitude, as well as zero-lag and lagged connectivity differences between the two groups.

For the replication analysis, we defined four ROIs in the cortical solution space using the centroid voxels reported in Elmer et al.'s study (2015; see Fig. 3-A). In each hemisphere, one ROI was placed in the auditory cortex (Brodmann Area [BA] 41/42, xyz coordinates in mm: $\pm 54, -25, 10$) and one ROI was placed in the DLPFC (BA 9/10/46, xyz coordinates in mm: $\pm 25, 45, 24$). As in the original study, EEG functional connectivity between the two ROIs in each hemisphere was evaluated in the theta frequency band (4–7 Hz).

For the exploratory whole-brain network analysis, we computed lagged phase synchronization, linear lagged connectivity, and linear instantaneous connectivity between the centroid voxels of all 84 BAs as

implemented in the sLoreta/eLoreta toolbox. Here, we included four frequency bands: theta (4–7 Hz), alpha (8–12 Hz), lower beta (13–21 Hz), and upper beta (22–30 Hz).

3.4. Data availability

Demographic and behavioral data, EEG raw data, EEG connectivity values, mean network values, and the networks found in the whole-brain analysis with all thresholds are available online at <https://dx.doi.org/10.17605/OSF.IO/HBZ28>.

3.5. Statistical analysis

We performed (1) statistical analyses of the demographic and behavioral data, (2) replication analyses of the EEG functional connectivity between the auditory cortex and the DLPFC, and (3) network-based analyses of whole-brain EEG functional connectivity.

If not otherwise specified, the analyses were performed using R (version 3.4.3; <https://www.r-project.org>; R Core Team, 2017). Frequentist Analyses of variance (ANOVAs) were computed using the R package ez (version 4.4.0; <https://cran.r-project.org/web/packages/ez/index.html>; Lawrence, 2016). Unless otherwise stated, the significance level α was set to 0.05. We report effect sizes as generalized eta-squared η^2_G (Bakeman, 2005) for ANOVAs and as Cohen's d (Cohen, 1988) for t -tests.

3.5.1. Statistical analyses of demographic and behavioral data

The musical aptitude test AMMA was analyzed with a 2×2 ANOVA with factors Group (AP and non-AP) and Score Subtype (tonal and rhythmical). All other participant characteristics and behavioral data were analyzed using two-tailed Welch's t -tests.

3.5.2. EEG ROI-based replication analyses

For the ROI-based replication analysis, we used both frequentist and Bayesian statistics. The frequentist analysis exactly replicated the statistical methods used in the original study (Elmer et al., 2015). However, frequentist analyses are limited in that they only permit the rejection of the null hypothesis (H_0) but not of the alternative hypothesis (H_1). Non-significant results cannot be interpreted as evidence for the absence of an effect. In contrast, Bayesian statistics quantify the evidence both for and against H_0 (Dienes, 2011, 2014; Lee and Wagenmakers, 2013; Rouder et al., 2009), which is especially useful for the interpretation of non-significant results (Dienes, 2014) and for the evaluation of replication success (Anderson and Maxwell, 2016). Thus, we computed Bayes factors in addition to the frequentist analysis. Bayes factors compare the (marginal) likelihood of the data under one hypothesis (e.g., H_0) with the (marginal) likelihood of the data under another hypothesis (e.g., H_1). The relative evidence for one hypothesis as expressed by a Bayes factor can be readily interpreted: A Bayes factor of $BF_{10} = 5$ (or the inverse $\frac{1}{BF_{10}} = BF_{01} = 0.2$) means that the data is five times more likely to occur under H_1 than under H_0 .

For the frequentist replication analyses, the lagged phase synchronization values were subjected to a 2×2 ANOVA with factors Group (AP and non-AP) and Hemisphere (left and right). We also computed a one-tailed Welch's t -test to specifically examine the group difference in the left hemisphere, in which the original study found higher connectivity in AP. In addition to the group statistics, we computed one-sided partial correlations for AP musicians between pitch-labeling accuracy and left hemispheric connectivity adjusted for the age of onset of musical training.

Bayes factors for Bayesian ANOVAs (BANOVAs), Bayesian t -tests, and Bayesian correlations were computed using the R package BayesFactor (version 0.9.12–4.2; <https://cran.r-project.org/web/packages/BayesFactor/index.html>; Morey et al., 2018). We used the default priors (a Cauchy distribution centered around zero with a scale

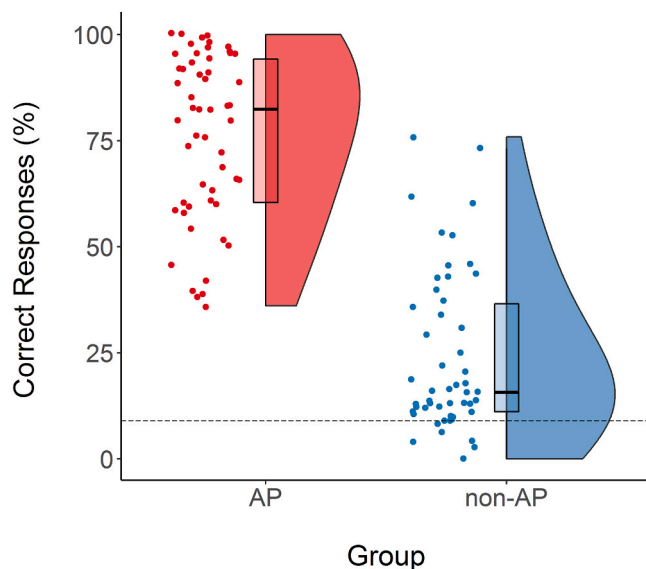


Fig. 2. Pitch-labeling scores for AP ($n = 54$) and non-AP ($n = 51$) musicians. Because octave errors were disregarded, the chance level was 8.33% (dashed line). Abbreviations: AP = absolute pitch.

parameter of 0.707) with the default number of iterations ($n = 10,000$). Since effect sizes are often inflated in studies with small sample sizes, we refrained from using scale-informed priors based on the effect sizes of the original study (Button et al., 2013; Halsey et al., 2015; Ioannidis, 2008). To confirm the robustness of the results, we tested a variety of additional priors with scale parameters between 0.5 (medium) and 1 (ultra-wide); the results suggested the same conclusions as reported here.

For the BANOVAs, Bayes factors of the two main effects (group and hemisphere) were assessed by comparing the model with one factor (e.g., group + subject) to the model with both factors (e.g., group + hemisphere + subject). Interaction effects were assessed by comparing the full model (group + hemisphere + group * deviation + subject) to the model without the interaction effect (group + hemisphere + subject). The Bayes factors reported for the one-sided correlation analyses do not account for the age of onset of musical training.

Extending the analyses of the original study, we analyzed two additional connectivity measures (lagged linear connectivity and instantaneous linear connectivity) to check whether the effect generalizes to other measures of functional connectivity. We report one-sided Welch's t -tests and Bayesian t -tests, and correlations for both hemispheres for all measures as described above.

3.5.3. EEG whole-brain network-based analyses

While the literature- and hypothesis-based definition of two centroids per hemisphere mitigates the multiple comparison problem, it carries the risk of missing other meaningful connections. For this reason, we additionally applied a less-restrictive, exploratory approach to investigate the resting-state EEG data. The whole-brain eLORETA output matrices (84 centroids of 84 BAs) were subjected to group comparisons using the network-based statistic (NBS) toolbox (Zalesky et al., 2010; <http://www.nitrc.org/projects/nbs/>) in MATLAB (version R2017b; <https://www.mathworks.com/products/matlab.html>). The analysis was performed separately for the four frequency bands of interest (theta, alpha, lower beta, and upper beta) and the three connectivity measures (lagged phase synchronization, lagged linear connectivity, and instantaneous linear connectivity). The NBS method provides a control for the family-wise error (FWE) rate when testing each connection between many ROIs. It applies the same principles as nonparametric cluster-based thresholding conventionally used in fMRI analyses (Nichols and Holmes, 2001). By considering interconnectedness in the topological space, NBS treats networks holistically and does not declare significance for individual connections.

To compare the individual connectivity matrices between the groups, we used the t -test module in NBS for both one-tailed contrasts (1, -1 and -1, 1). First, this module computed t -test statistics for each pairwise association between the 84 ROIs. Edges exceeding a specified threshold formed a suprathreshold network if connected with each other. The size (i.e., the number of edges) of the largest observed suprathreshold network was subjected to permutation testing. For a total of 5000 permutations, the group labels of the participants were randomly exchanged, and the analysis was repeated using the same threshold. From each permutation step, the size of the largest suprathreshold network was stored to form an empirical estimate of the null distribution. The p -value of the observed network was estimated by counting the permutations that yielded the same or a bigger maximal network size and dividing this count by the total number of permutations. Thus, the reported p -values are FWE corrected only for the number of ROIs. We applied no additional correction for the number of NBS tests performed because of the exploratory nature of the analysis (Althouse, 2016; Bender and Lange, 2001).

Because we were interested in middle ($d \approx 0.4$) to large ($d \approx 0.8$) effect sizes on the level of individual links, we tested the connectivity matrices for the corresponding thresholds between $t = 2.0$ and $t = 4.0$ in increments of 0.1. For each separate analysis (four frequency bands, three connectivity measures, two contrasts), we report all thresholds at

which a network with $p < .05$ emerged. We describe one of these networks in detail, which is representative of the networks obtained using those thresholds. All networks with $p < .05$ are available online at <https://dx.doi.org/10.17605/OSF.IO/HBZ28>. The reported networks were visualized using the BrainNet Viewer software (version 1.53; <http://www.nitrc.org/projects/bnv/>) in MATLAB (Version R2017b, <https://www.mathworks.com/products/matlab.html>). The Harvard-Oxford cortical atlas and the Juelich Histological atlas as implemented in FSL (<http://fsl.fmrib.ox.ac.uk/fsl/fslwiki/FSL>) were used to specify the brain regions underlying the involved nodes.

After identification of the networks, we analyzed the relationship between the corresponding mean network values and pitch-labeling performance using R (version 3.4.3; <https://www.r-project.org>; R Core Team, 2017). We computed both frequentist and Bayesian correlations (two-sided, non-partial) for each group separately.

4. Results

4.1. Results of demographic and behavioral analyses

AP and non-AP musicians were comparable in age ($t_{(100.97)} = 1.33$, $p = .19$, $d = 0.26$), intelligence ($t_{(102.86)} = -1.49$, $p = .14$, $d = 0.29$), age of onset of musical training ($t_{(102.42)} = -1.20$, $p = .23$, $d = 0.23$), and cumulative musical training hours over the lifespan ($t_{(99.71)} = 1.43$, $p = .16$, $d = 0.28$). The analysis of the AMMA scores (measuring musical aptitude) yielded a main effect of Group ($F_{(1,103)} = 4.60$, $p = .034$, $\eta_G^2 = 0.04$), a main effect of Score Subtype ($F_{(1,103)} = 79.27$, $p < .001$, $\eta_G^2 = 0.07$), and an interaction effect ($F_{(1,103)} = 5.37$, $p = .023$, $\eta_G^2 = 0.005$). Post hoc t -tests (Bonferroni corrected $\alpha = 0.25$) revealed that the AP musicians were comparable to non-AP musicians in the rhythmical score ($t_{(101.38)} = 1.53$, $p = .13$, $d = 0.30$) but had a higher tonal score ($t_{(100.61)} = 2.44$, $p = .016$, $d = 0.48$). As expected, AP musicians outperformed non-AP musicians in the pitch-labeling task ($t_{(102.93)} = 13.95$, $p < .001$, $d = 2.72$; see Fig. 2).

4.2. Results of ROI-based replication analyses

The ROI-based replication analysis of lagged phase synchronization – the measure used in the original study (Elmer et al., 2015) – in the theta frequency band between the auditory cortex and the DLPFC revealed no evidence for a main effect of Group ($F_{(1,103)} = 1.86$, $p = .18$, $\eta_G^2 = 0.01$, $BF_{01} = 3.39$), no evidence for a main effect of Hemisphere ($F_{(1,103)} = 0.06$, $p = .81$, $\eta_G^2 < 0.001$, $BF_{01} = 8.90$), and no evidence for a Group \times Hemisphere interaction ($F_{(1,103)} = 0.01$, $p = .91$, $\eta_G^2 < 0.001$, $BF_{01} = 6.69$). Lagged-synchronization values are shown in Fig. 3-B and posterior distributions of the BANOVA are illustrated in Fig. 3-D. The planned one-tailed t -test did not reveal evidence for a difference between the two groups in the left hemisphere ($t_{(102.75)} = -0.90$, $p = .81$, $d = 0.18$, $BF_{01} = 8.49$; see Fig. 3-B). There was also no evidence for a positive relationship between pitch-labeling performance and left-hemispheric lagged phase synchronization in AP musicians ($r_p = -0.034$, $p = 1.00$, $BF_{01} = 4.26$; see Fig. 3-C).

Additional analyses of resting-state connectivity between the auditory cortex and the DLPFC in AP musicians based on lagged linear connectivity and instantaneous linear connectivity also revealed no evidence for differences between the two groups. All results of the group comparisons for each hemisphere are shown in detail in Table 2. There was also no evidence for a positive relationship between pitch-labeling performance and resting-state connectivity between the auditory cortex and the DLPFC in AP musicians. The results of the correlational analyses are shown in Table 3.

4.3. Results of whole-brain network-based analyses

The network-based analyses of the 84-ROI connectivity matrices revealed group differences in three measure \times frequency combinations

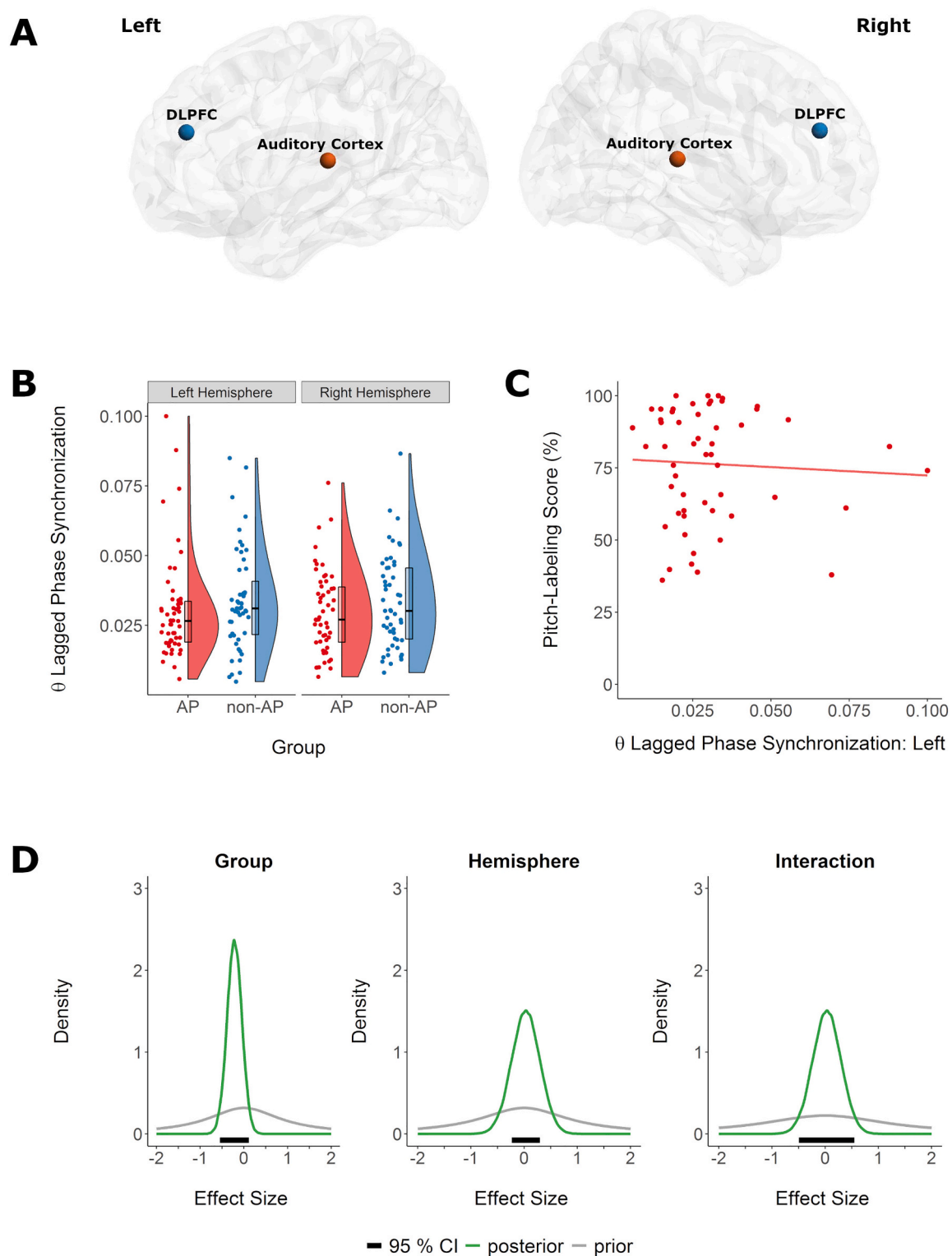


Fig. 3. Replication analysis of theta lagged phase synchronization between the auditory cortex and the DLPFC during EEG resting state. A) Localization of the four ROIs. B) There was no evidence for a difference in theta lagged phase synchronization values between AP musicians (red) and non-AP musicians (blue). C) There was no evidence for a positive correlation between left-hemispheric theta lagged phase synchronization and performance in the pitch-labeling task in AP musicians. D) Prior (gray) and posterior (green) distributions of the standardized effects (relative to the standard deviation of the error term) of the factors Group and Hemisphere on theta lagged phase synchronization. The Bayesian 95% credible interval describes the interval that includes the true value with a probability of 95%, given the data and the assumed model. Abbreviations: 95% CI = Bayesian 95% credible interval, AP = absolute pitch, DLPFC = dorsolateral prefrontal cortex, ROI = region of interest. (For interpretation of the references to color in this figure legend, the reader is referred to the web version of this article.)

(see Fig. 4): AP musicians showed hyperconnected resting-state networks in (A) lagged linear connectivity in lower beta, (B) in instantaneous linear connectivity in lower beta, and (C) in instantaneous

linear connectivity in theta. No networks with $p < .05$ were observed in lagged phase synchronization or in any of the other tested frequency bands of lagged and instantaneous linear connectivity. The analyses did

Table 2

Group comparisons of theta-band connectivity between the auditory cortex and the DLPFC.

Connectivity Measure	Hemisphere	AP	Non-AP	<i>p</i> -value	Cohen's <i>d</i>	BF ₀₁
Lagged phase synchronization	Right	0.030 (0.015)	0.033 (0.017)	0.88	0.23	9.77
	Left	0.030 (0.018)	0.034 (0.018)	0.81	0.18	8.49
Lagged linear connectivity	Right	0.046 (0.029)	0.049 (0.031)	0.70	0.11	6.96
	Left	0.043 (0.028)	0.051 (0.032)	0.91	0.27	10.64
Instantaneous linear connectivity	Right	0.967 (0.773)	0.810 (0.466)	0.10	0.25	1.37
	Left	0.787 (0.415)	0.756 (0.433)	0.35	0.07	3.55

Annotations. One-sided Welch's *t*-tests were applied to compare AP and non-AP musicians (hypothesis AP > non-AP). Group values for AP and non-AP musicians are given as mean (standard deviation in parentheses). Lagged phase synchronization was the measure used in the original study (Elmer et al., 2015). Abbreviations: AP = absolute pitch, DLPFC = dorsolateral prefrontal cortex.

Table 3

Correlations between pitch-labeling performance and theta-band connectivity in AP musicians.

Connectivity measure	Hemisphere	<i>r</i>	<i>p</i> _{one-sided}	BF ₀₁
Lagged phase synchronization	Right	0.160	0.12	0.99
	Left	−0.034	1.00	4.26
Lagged linear connectivity	Right	0.001	0.50	2.49
	Left	−0.157	1.00	3.86
Instantaneous linear connectivity	Right	−0.199	1.00	6.70
	Left	−0.054	1.00	3.86

Annotations. One-sided partial correlations (*r* and *p* adjusted for age of onset of musical training; hypothesis higher pitch-labeling score is associated with stronger connectivity). Theta-band connectivity was evaluated between the auditory cortex and the DLPFC. Lagged phase synchronization was the measure used in the original study (Elmer et al., 2015). Abbreviations: AP = absolute pitch, DLPFC = dorsolateral prefrontal cortex.

also not reveal any networks with decreased connectivity in AP musicians compared to non-AP musicians.

(A) In lagged linear connectivity in the lower beta frequency band, networks with $p < .05$ were found for all tested thresholds between $t = 2.0$ (76 nodes, 423 edges) and $t = 3.7$ (2 nodes, 1 edge). We report the network at $t = 3.0$, visualized in Fig. 4-A. At this threshold, 13 nodes and 14 edges contributed to the network ($p = .037$, FWE corrected for the number of ROIs). The brain regions underlying the involved nodes are listed in Table 4. Nodes in the left temporal lobe (auditory regions, planum temporale) were connected to nodes in the frontal lobe both intrahemispherically (left middle and superior frontal gyrus) and interhemispherically (right middle/ superior frontal gyrus, BA 6). Within the right hemisphere, nodes in the frontal lobe (middle frontal gyrus, superior frontal gyrus, inferior frontal gyrus), in the parietal operculum, in the insular cortex, and in the middle temporal gyrus contributed to the network. Two-sided correlations revealed no evidence for a relationship between mean network values and pitch-labeling performance within AP musicians ($r = 0.095$, $p = .49$, BF₀₁ = 2.63) or within non-AP musicians ($r = 0.075$, $p = .60$, BF₀₁ = 2.80).

(B) In instantaneous linear connectivity in the lower beta frequency band, networks with $p < .05$ were obtained at thresholds between $t = 2.0$ (77 nodes, 411 edges) and $t = 3.0$ (19 nodes, 23 edges), and at $t = 3.6$ (4 nodes, 3 edges) and $t = 3.7$ (3 nodes, 2 edges). The relatively widespread network at $t = 3.0$ ($p = .044$, FWE corrected for number of ROIs; see Table 5 and Fig. 4 B) consisted of nodes in the occipital lobe (visual cortex, occipital pole, precuneus), in subcortical regions (hippocampal and parahippocampal regions), in the temporal lobe (inferior temporal gyrus, middle temporal gyrus, temporal pole, planum temporale/auditory cortex), and in the frontal lobe (frontal pole, inferior

frontal gyrus). There was no evidence for a correlation between mean network values and pitch-labeling performance within the AP group ($r = 0.004$, $p = .97$, BF₀₁ = 3.25) or within the non-AP group ($r = 0.008$, $p = .96$, BF₀₁ = 3.17).

(C) In instantaneous linear connectivity in the theta frequency band, NBS revealed networks with $p < .05$ at thresholds between $t = 3.1$ (11 nodes, 15 edges) and $t = 3.5$ (7 nodes, 6 edges). At a middle-level threshold of $t = 3.3$, the network ($p = .032$, FWE corrected for number of ROIs) comprised of 8 nodes in temporal and perisylvian regions (middle temporal gyrus, superior temporal gyrus, planum temporale, auditory cortex, and parietal operculum) and of 10 interhemispheric connections. The network nodes are described in detail in Table 6, and the network is visualized in Fig. 4-C. Similar to the other two networks, there was no evidence for a relationship between mean network values and pitch-labeling performance in either AP ($r = 0.070$, $p = .63$, BF₀₁ = 2.92) or non-AP musicians ($r = -0.16$, $p = .27$, BF₀₁ = 1.83).

5. Discussion

This study investigated EEG resting-state connectivity in AP and non-AP musicians to provide insights into the role of perceptual and cognitive processes in AP. In a two-part analysis, we first attempted to replicate our previous finding of increased theta resting-state connectivity between the left auditory cortex and the left DLPFC (Elmer et al., 2015). In the second part, we performed an exploratory whole-brain analysis to evaluate whether the auditory cortex and the DLPFC are part of a larger AP-specific resting-state network.

In the ROI-based replication analysis, we found no evidence for an increase in theta-band lagged phase synchronization between the auditory cortex and the DLPFC in AP musicians compared to non-AP musicians. Bayes factor analyses favored the null hypothesis of no group differences (BF > 8). Similar results were obtained for two additionally analyzed connectivity measures. There was also no evidence for a positive relationship between pitch-labeling proficiency and left-hemispheric theta connectivity in the AP group. The whole-brain analysis provided weak evidence in favor of hyperconnected networks in AP musicians in the theta and lower-beta frequency bands using instantaneous linear connectivity, and in the lower-beta frequency band using lagged linear connectivity.

5.1. ROI-based replication analyses: auditory cortex and DLPFC

In the ROI-based analysis, we did not replicate the previous finding (Elmer et al., 2015) of increased left-hemispheric temporo-frontal connectivity in AP musicians. This corresponds at least partly with previous reports on functional connectivity in AP. While the connectivity of the auditory cortex in AP has been addressed by several

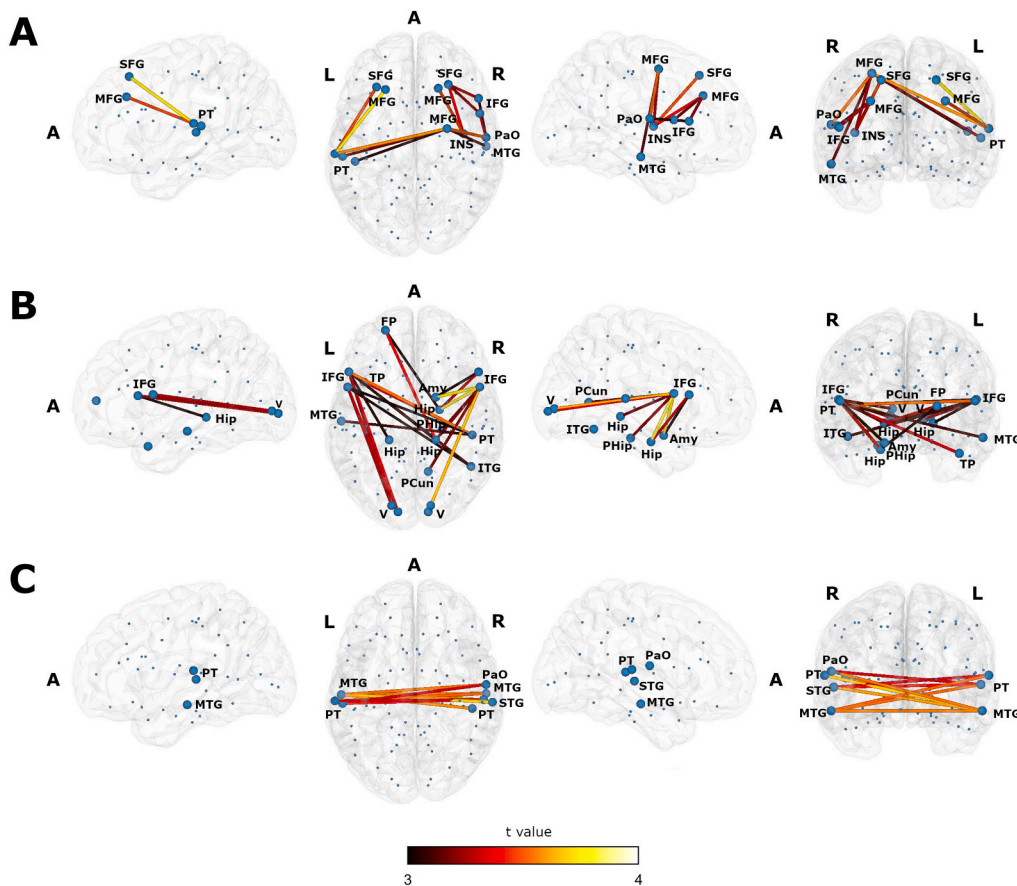


Fig. 4. Lateral, axial and coronal views of the three obtained resting-state networks. All three networks show increased undirected connectivity in AP musicians compared to non-AP musicians. Blue spheres represent the centroids of the 84 Brodmann Areas. Nodes contributing to the network are depicted by enlarged spheres. The color of the edges corresponds to the *t*-value. A) The network in lagged linear connectivity in lower beta. B) The network in instantaneous linear connectivity in lower beta. C) The network in instantaneous linear connectivity in theta.

Abbreviations: A = anterior, Amy = amygdala, AP = absolute pitch, FP = frontal pole, Hip = hippocampus subiculum, IFG = inferior frontal gyrus, INS = insular cortex, ITG = inferior temporal gyrus, L = left hemisphere, MFG = middle frontal gyrus, MTG = middle temporal gyrus, PaO = parietal operculum, PCun = precuneus cortex, PHip = parahippocampal gyrus, PT = planum temporale, R = right hemisphere, SFG = superior frontal gyrus, STG = superior temporal gyrus, TP = temporal pole, V = visual cortex. (For interpretation of the references to color in this figure legend, the reader is referred to the web version of this article.)

previous studies (e.g., Jäncke et al., 2012; Loui et al., 2011, 2012), much less is known about the DLPFC. For instance, a recent functional magnetic resonance imaging (fMRI) study found differential local connectivity patterns in the left auditory cortex during resting state but neither local nor global connectivity differences in the DLPFC between musicians with and without AP (Brauchli et al., 2019a). In another fMRI study, the Heschl's gyrus was functionally connected to various auditory and non-auditory regions during passive tone listening in the AP group (Wengenroth et al., 2014). However, no evidence was found for an AP-specific synchronization between the auditory cortex and the DLPFC. Furthermore, Kim and Knösche (2017b) found no evidence for group differences in resting-state connectivity between the auditory cortex and seeds in the planum temporale, which is part of the dorsal

auditory pathway between the auditory cortex and the DLPFC (Rauschecker and Scott, 2009). Alternatively, it has been proposed that the ventral pathway projecting to the inferior frontal gyrus via the anterior temporal lobe might play a more important role in AP processing than the DLPFC (Kim and Knösche, 2017a, 2017b; Leipold et al., 2019b). The only other study besides Elmer et al. (2015) providing some evidence for the importance of a dorsal connection between auditory and frontal regions in AP found a leftward asymmetry of fractional anisotropy measures of the arcuate fasciculus in AP musicians but not in non-AP musicians or non-musicians (Oechslin et al., 2010a). The arcuate fasciculus structurally connects the posterior superior temporal gyrus and the prefrontal cortex (Makris et al., 2005). Taken together, there is not yet much support for increased connectivity between the

Table 4

Brain regions underlying the centroid voxel coordinates of the BAs constituting the lower-beta linear lagged connectivity network (*t* threshold = 3.0 associated with a Cohen's *d* = 0.59).

MNI coordinates (x, y, z)	Brain region	Brodmann area
−22, 28, 49	left superior frontal gyrus	BA 8
−29, 30, 33	left middle frontal gyrus	BA 9
−56, −25, 5	left planum temporale/primary auditory cortex	BA 41
−46, −29, 10	left planum temporale/primary auditory cortex	BA 41
−62, −23, 12	left planum temporale	BA 42
27, −3, 54	right middle frontal gyrus/superior frontal gyrus	BA 6
20, 29, 49	right superior frontal gyrus	BA 8
28, 32, 33	right middle frontal gyrus	BA 9
40, −7, 9	right insular cortex	BA 13
58, −17, −15	right middle temporal gyrus	BA 21
58, −10, 15	right secondary somatosensory cortex/parietal operculum	BA 42
53, 9, 14	right inferior frontal gyrus (Broca's area BA44)	BA 44
52, 21, 13	right inferior frontal gyrus (Broca's area BA44/BA45)	BA 44/45

Annotations. Nodes were assigned to brain regions based on the Harvard-Oxford cortical atlas and the Juelich Histological atlas. Brodmann areas refer to the LORETA output. Abbreviations: BA = Brodmann area.

Table 5

Brain regions underlying the centroid voxel coordinates of the BAs constituting the lower-beta linear instantaneous connectivity network (t threshold = 3.0 associated with a Cohen's d = 0.59).

MNI coordinates (x, y, z)	Brain region	Brodman area
–22, 54, 9	left frontal pole	BA 10
–12, –90, –1	left visual cortex (V1, V2, V3)/occipital pole	BA 17
–17, –85, 1	left visual cortex (V3)	BA 17
–57, –18, –15	left middle temporal gyrus	BA 21
–19, –33, –4	left hippocampus subiculum	BA 27
–39, 13, –27	left temporal pole	BA 38
–52, 9, 14	left inferior frontal gyrus (Broca's area BA44)	BA 44
–51, 21, 13	left inferior frontal gyrus (Broca's area BA44)	BA 44/45
12, –90, 0	right visual cortex (V1)/occipital pole	BA 17
14, –85, 2	right visual cortex (V1)	BA 17
18, –33, –4	right hippocampus subiculum	BA 27
21, –9, –24	right hippocampus subiculum	BA 28
12, –58, 7	right visual cortex (V1)/precuneus cortex	BA 30
18, 1, –19	right amygdala superficial group/parahippocampal gyrus	BA 34
23, –25, –21	right parahippocampal gyrus	BA 35
46, –54, –14	right inferior temporal gyrus/temporal occipital fusiform cortex	BA 37
47, –29, 10	right planum temporale/primary auditory cortex	BA 41
53, 9, 14	right inferior frontal gyrus (Broca's area BA44)	BA 44
52, 21, 13	right inferior frontal gyrus (Broca's area BA44/BA45)	BA 44/45

Annotations. Nodes were assigned to brain regions based on the Harvard-Oxford cortical atlas and the Juelich Histological atlas. Brodmann areas refer to the LORETA output. Abbreviations: BA = Brodmann area.

Table 6

Brain regions underlying the centroid voxel coordinates of the BAs constituting the theta linear instantaneous connectivity network (t threshold = 3.3 associated with a Cohen's d = 0.65).

MNI coordinates (x, y, z)	Brain region	Brodman area
–57, –18, –15	left middle temporal gyrus	BA 21
–56, –25, 5	left planum temporale/primary auditory cortex	BA 41
–62, –23, 12	left planum temporale	BA 42
58, –17, –15	right middle temporal gyrus	BA 21
56, –22, 3	right superior temporal gyrus	BA 41
47, –29, 10	right planum temporale/primary auditory cortex	BA 41
63, –24, 12	right planum temporale	BA 42
58, –10, 15	right secondary somatosensory cortex/parietal operculum	BA 42

Annotations. Nodes were assigned to brain regions based on the Harvard-Oxford cortical atlas and the Juelich Histological atlas. Brodmann areas refer to the LORETA output. Abbreviations: BA = Brodmann area.

auditory cortex and the DLPFC in AP, consistent with the results of the current study.

Some studies suggested that the DLPFC might be involved in the pitch-label association process in AP (Bermudez and Zatorre, 2005; Levitin and Rogers, 2005; Ohnishi et al., 2001; Zatorre et al., 1998). However, a recent fMRI study of our group did not observe an involvement of the DLPFC in AP during a pitch-processing task (Leipold et al., 2019a), casting doubt on the exact role of the DLPFC in pitch labeling. Activity in the DLPFC increased equally in musicians with and without AP between a listening and a labeling condition. Hence, we suggested that the activity in the DLPFC might actually reflect unspecific attentional or executive control processes rather than the label retrieval itself. The inconsistencies in DLPFC activation even during acoustic stimulation might explain to some extent why the increase in functional connectivity between the left auditory cortex and the left DLPFC could not be reliably detected during EEG resting state.

It is important to note that the DLPFC encompasses a rather large cortex region whose exact location and extension are not universally agreed upon (e.g., BA 9/46 Cieslik et al., 2013; BA 8/9/46 O'Reilly, 2010; BA 8/9/46 Plakke and Romanski, 2014; BA 8a/46 Rauschecker, 2011; BA 9/10/46 Teffer and Semendeferi, 2012). By considering only

a single centroid within the DLPFC in our replication analysis, we cannot make statements about this broad region as a whole. We can only conclude that there was no evidence for an AP-specific increase in connectivity between the auditory cortex and the DLPFC as it was defined in the original study.

5.2. Whole-brain network-based analyses

The exploratory whole-brain analyses yielded three resting-state networks with enhanced EEG connectivity (i.e., hyperconnectivity) in AP musicians compared to non-AP musicians. We did not find any evidence for networks with decreased connectivity in AP musicians. Several MRI studies have reported functional and structural hyperconnectivity in AP using a variety of both ROI-based and whole-brain methods (Brauchli et al., 2019a; Dohn et al., 2015; Kim and Knösche, 2017b; Loui et al., 2011, 2012; Wengenroth et al., 2014). On the other hand, there is also one report of reduced whole-brain connectivity (i.e., cortical thickness covariance) in AP musicians (Jäncke et al., 2012). Similarly, a recent EEG resting-state study observed global hypoconnectivity (i.e., lower clustering) in AP musicians on the electrode level (Wenhardt et al., 2019). A recently published source-level EEG study, however, did not find any evidence for network differences between AP and non-AP musicians during resting state (Brauchli et al., 2019b). In contrast to our study, Brauchli and colleagues analyzed eyes-open instead of eyes-closed resting-state data. Taken together, there is some heterogeneity in the literature as to whether connectivity in AP musicians is increased, decreased, or comparable to non-AP musicians. The greatly varying methods (e.g., imaging modality, structural vs functional, ROI-based vs whole-brain, electrode-level vs source-level, eyes-open vs eyes-closed, dependency measures, different types of connectivity and network analyses, different procedures for AP group assignment) may account for some of the diverging results. Resting-state connectivity of AP musicians might in particular be affected by the imaging modality. In addition to the inherent differences between fMRI and EEG regarding temporal and spatial resolution, there is no background noise during EEG recording. The fMRI scanner noise, on the other hand, might activate some pitch-labeling processes in AP musicians. Further research is necessary to disentangle hyper- and hypoconnectivity in AP and the influence of the respectively used methods.

The three networks we identified in our exploratory whole-brain analysis covered nodes in frontal, temporal, subcortical, and occipital

brain regions. Common features across the three networks were the planum temporale, the inferior frontal gyrus, the parietal operculum, and the middle temporal gyrus. The planum temporale, a secondary auditory region posterior to the Heschl's gyrus, has repeatedly been associated with AP (Burkhard et al., 2020; Keenan et al., 2001; Leipold et al., 2019a; Luders et al., 2004; Ohnishi et al., 2001; Schlaug et al., 1995; Wengenroth et al., 2014; Wilson et al., 2009; Zatorre et al., 1998). While its precise function in AP remains unknown, the planum temporale has been suspected to be involved in the matching of auditory input to internal templates (Griffiths and Warren, 2002). As recently put forward by Leipold et al., 2019a, a similar matching process specifically involving pitch templates might occur in the planum temporale of AP musicians during pitch labeling. The parietal operculum (secondary somatosensory cortex) has also been previously reported in connection with AP; its involvement was presumed to indicate sensorimotor integration (Wengenroth et al., 2014). However, considering the relatively low spatial resolution of EEG and the spatial closeness of the centroid voxels of the parietal operculum and the planum temporale, these nodes might not necessarily show selective neural activations of different brain regions in the present study. The inferior frontal gyrus has repeatedly been implicated in AP (Dohn et al., 2015; Leipold et al., 2019a; McKetton et al., 2019; Schulze et al., 2009; Wengenroth et al., 2014; Zatorre et al., 1998). Because its activity was either increased or decreased in AP musicians depending on the specific task, different functions have been attributed to it, such as a verbal component in AP processing (Wengenroth et al., 2014) or a working memory component in relative-pitch processing (Leipold et al., 2019a). Finally, the middle temporal gyrus has also been previously linked to AP (Burkhard et al., 2019; Kim and Knösche, 2017b; Loui et al., 2011; Wengenroth et al., 2014; Zatorre et al., 1998). The middle temporal gyrus participates in a multitude of functions (for an overview, consider Xu et al., 2015), including higher-order language processes (Friederici, 2002; Hickok and Poeppel, 2007; Oechslin et al., 2010b). In the context of AP, the middle temporal gyrus has been proposed to play a role in accessing stored pitch templates (Loui et al., 2012), in categorizing perceived tones (Burkhard et al., 2019), or in recruiting multimodal codes for extracted pitch information (Zatorre et al., 1998).

The networks were found in the theta (4–7 Hz) and the lower-beta (13 Hz – 21 Hz) frequency range. A number of cognitive functions have been linked to these oscillation rhythms (for a review, see Wang, 2010). For theta, these functions include working memory, memory encoding, and memory retrieval (Albouy et al., 2017; Hsieh and Ranganath, 2014; Ward, 2003), whereas the beta frequency band is involved in sensorimotor integration and top-down signaling (Engel and Fries, 2010; Siegel et al., 2012). These attributed functions are very well in accordance with the brain regions we found contributing to the AP-specific networks.

For all three networks, we found no evidence for a relationship between the mean network connectivity values and pitch-labeling scores within the group of AP musicians. Similarly, a recent fMRI resting-state study from our research project showed no significant correlations between the connectivity measures and pitch-labeling scores within the AP group (Brauchli et al., 2019a). As argued there with reference to a large-scale behavioral study (Athos et al., 2007), a possible explanation for this lack of correlation might be that AP is a distinct rather than a continuous ability. Another possibility is that even within the AP group, different strategies were used to solve the pitch-labeling task. Such individual differences beyond a common mechanism might explain the rather large variance in pitch-labeling scores within the AP musicians and, consequently, the lack of correlation with the network values. Finally, in light of the number of tests performed, it is also possible that the identification of the networks is affected by the type I error, and as a result, the mean network values do not significantly correlate with the pitch-labeling scores.

Overall, the nodes shared among the three networks corroborate the importance of perisylvian areas in AP, including prefrontal regions. The

non-overlapping nodes of the networks might indicate the use of a widespread, possibly multisensory network. However, considering the number of exploratory NBS analyses that did not yield any evidence for group differences, the strength of evidence for hyperconnectivity during eyes-closed resting-state EEG remains weak.

5.3. Limitations

Several general limitations apply to both the ROI-based and the whole-brain analysis. First, EEG source localization might be relatively imprecise when based on a small number of electrodes (Baillet, 2017; Srinivasan et al., 1998). To be sufficiently confident of the source reconstruction, we checked localization accuracy during acoustic stimulation, which confirmed that the eLORETA algorithm performed well on our data. Additionally, previous studies have verified the source reconstruction accuracy of the LORETA toolbox even for small numbers of scalp electrodes using intracranial electrode recording (Zumsteg et al., 2005, 2006). Second, the connectivity measures used in the analyses do not distinguish between direct and indirect connections (common input problem: Bastos and Schoffelen, 2016). Thus, connectivity between two nodes could have been mediated by a third source not included in the analysis. Lastly, caution must be applied when generalizing resting-state networks to active processing. As pointed out by Petersen and Sporns (2015), it could be that even brain networks activated by daily tasks (e.g., reading) are not necessarily expressed during resting state if, for instance, the contributing regions are also used by various other tasks. Thus, future connectivity analyses during active tasks are vital for a better understanding of the networks specifically involved in the process of pitch labeling in AP.

Additional limitations specifically apply to the ROI-based replication analysis. While both the current and the original study relied on self-reports with respect to group assignment to the AP and non-AP groups and retrospectively tested this group assignment using a pitch-labeling test, there are still some differences in terms of the used samples. First, we changed the assessment of the questionnaires and the pitch-labeling task from paper-pencil to online at home to lower the on-site testing workload for our participants. Second, due to the online implementation, the pitch-labeling task had to be slightly modified: Trials could last up to 15 s instead of a fixed duration of 5 s in the paper-pencil implementation of the original study. A pilot test showed that this modification was necessary for participants to be able to solve the multiple-choice format with 36 response options. Third, contrary to the original study, AP musicians scored higher than non-AP musicians in the tonal part of the musical aptitude test (AMMA) in the present study. Whilst statistically significant, this group difference was small in absolute numbers (less than 2 points out of a maximal score of 40 points), and the means were similar to those of the original sample. Finally, there was no overlap between the two groups in pitch-labeling scores in the original study (all non-AP musicians had less than 20% correct, all AP-musicians had more than 35% correct), but there was an overlap in our sample (highest score among non-AP musicians was 75.9%, the lowest score among AP musicians was 36.1%). This could be attributed to less homogenous groups but might also be due to the larger sample size or the longer trial duration in our pitch-labeling task: Because the participants had more time to respond, they might have used their relative-pitch ability to solve the task. It is conceivable that highly trained non-AP musicians can perform well under these circumstances. The difference between the two studies regarding the overlap in pitch-labeling scores seems to mostly stem from such well-performing non-AP musicians in the current study. To prevent non-AP musicians from using relative-pitch cues in pitch-labeling tasks, future studies should consider using non-harmonic and distorted interference stimuli between the tones as proposed by Wengenroth et al. (2014). AP musicians showed a similarly large range of pitch-labeling scores in the current and the original study. Unpublished data from our lab suggests a strong correlation ($r = 0.77$) between the online pitch-labeling test used in the

current study and the on-site test used in the original study within AP musicians ($n = 39$). Although this correlation is strong there is still some unexplained variance, which might indicate that different cognitive functions have been involved during the performance of these different pitch-labeling task variants. Whether these suspected differences between the previous and the current study might be responsible for the different findings is disputable and should be examined in further experiments. We also found no evidence for a positive correlation between the pitch-labeling scores and the connectivity values of the ROI-based analysis within the AP group, which would have supported the importance of the connection between the auditory cortex and the DLPFC for AP.

5.4. Conclusion

Using the ROIs defined in Elmer et al.'s (2015) study, we did not replicate an AP-specific increase in resting-state connectivity between the auditory cortex and the DLPFC in the theta frequency band. The exploratory whole-brain analyses provided weak evidence for increased functional interactions among distributed brain areas in AP in the theta and lower-beta frequency bands. These areas comprised mainly auditory and frontal brain regions but also included regions that engage in sensorimotor and visual processes. Future task-based studies using acoustic stimulation are necessary to confirm the involvement of these regions and to clarify their specific role in the pitch-labeling process.

Funding sources

This work was funded by the Swiss National Science Foundation (SNSF), grant number 320030_163149 to LJ.

Author contributions

S.L., M.G., C.K., and L.J. designed research; M.G. performed research; M.G., and S.S. analyzed data; M.G., S.L., S.S., C.K., and L.J. wrote the paper.

Declaration of competing interest

The authors declare no conflict of interest.

Acknowledgements

We are particularly grateful to Stefan Elmer for his support. His research has inspired this work greatly. We also wish to thank our research interns and research assistants Anna Speckert, Chantal Oderbolz, Fabian Demuth, Florence Bernays, Isabel Hotz, Joëlle Albrecht, Kathrin Baur, Laura Keller, Melek Haçan, Nicole Hedinger, Pascal Misala, Petra Meier, Piyush Rauch, Sarah Appenzeller, Tenzin Dotschung, Valerie Hungerbühler, Vanessa Vallesi, and Vivienne Kunz for their invaluable assistance with data collection. We thank Christian Brauchli and Anja Burkhard for their contributions within the larger project on absolute pitch.

References

- Albouy, P., Weiss, A., Baillet, S., Zatorre, R.J., 2017. Selective entrainment of theta oscillations in the dorsal stream causally enhances auditory working memory performance. *Neuron* 94, 193–206.
- Althouse, A.D., 2016. Adjust for multiple comparisons? It's not that simple. *Ann. Thorac. Surg.* 101, 1644–1645.
- Athos, E.A., Levinson, B., Kistler, A., Zemansky, J., Bostrom, A., Freimer, N.B., Gitschier, J., 2007. Dichotomy and perceptual distortions in absolute pitch ability. *Proc. Natl. Acad. Sci. U. S. A.* 104 (37), 14795–14800. <https://doi.org/10.1073/pnas.0703868104>.
- Anderson, S.F., Maxwell, S.E., 2016. There's more than one way to conduct a replication study: beyond statistical significance. *Psychol. Methods* 21, 1–12.
- Annett, M., 1970. A classification of hand preference by association analysis. *Br. J. Psychol.* 61, 303–321.
- Baillet, S., 2017. Magnetoencephalography for brain electrophysiology and imaging. *Nat. Neurosci.* 20, 327–339.
- Bakeman, R., 2005. Recommended effect size statistics for repeated measures designs. *Behav. Res. Methods* 37, 379–384.
- Bastos, A.M., Schoffelen, J.M., 2016. A tutorial review of functional connectivity analysis methods and their interpretational pitfalls. *Front. Syst. Neurosci.* 9, 1–23.
- Bender, R., Lange, S., 2001. Adjusting for multiple testing—when and how? *J. Clin. Epidemiol.* 54, 343–349.
- Bermudez, P., Zatorre, R.J., 2005. Conditional associative memory for musical stimuli in nonmusicians: implications for absolute pitch. *J. Neurosci.* 25, 7718–7723.
- Brauchli, C., Leipold, S., Jäncke, L., 2019a. Univariate and multivariate analyses of functional networks in absolute pitch. *Neuroimage*. <https://doi.org/10.1016/j.neuroimage.2019.01.021>.
- Brauchli, C., Leipold, S., Jäncke, L., 2019b. Diminished large-scale functional brain networks in absolute pitch during the perception of naturalistic music and audiobooks. *Neuroimage* 116513.
- Bressler, S.L., Menon, V., 2010. Large-scale brain networks in cognition: emerging methods and principles. *Trends Cogn. Sci.* 14, 277–290.
- Burkhard, A., Elmer, S., Jäncke, L., 2019. Early tone categorization in absolute pitch musicians is subserved by the right-sided perisylvian brain. *Sci. Rep.* 9, 1419.
- Burkhard, A., Hänggi, J., Elmer, S., Jäncke, L., 2020. The importance of the fibre tracts connecting the planum temporale in absolute pitch possessors. *Neuroimage* 211, 116590.
- Button, K.S., Ioannidis, J.P.A., Mokrysz, C., Nosek, B.A., Flint, J., Robinson, E.S.J., Munafò, M.R., 2013. Power failure: why small sample size undermines the reliability of neuroscience. *Nat. Rev. Neurosci.* 14, 365–376.
- Cieslik, E.C., Zilles, K., Caspers, S., Roski, C., Kellermann, T.S., Jakobs, O., Langner, R., Laird, A.R., Fox, P.T., Eickhoff, S.B., 2013. Is there one DLPFC in cognitive action control? Evidence for heterogeneity from co-activation-based parcellation. *Cereb. Cortex* 23, 2677–2689.
- Cohen, J., 1988. *Statistical Power Analysis for the Behavioral Science*, 2nd ed. Erlbaum, Hillsdale, NJ.
- Deutsch, D., 2013. 5 - Absolute Pitch. In: Deutsch, D. (Ed.), *The Psychology of Music*, Third edition. Academic Press, pp. 141–182.
- Dienes, Z., 2011. Bayesian versus orthodox statistics: which side are you on? *Perspect. Psychol. Sci.* 6, 274–290.
- Dienes, Z., 2014. Using Bayes to get the most out of non-significant results. *Front. Psychol.* 5, 781.
- Dohn, A., Garza-Villarreal, E.A., Chakravarty, M.M., Hansen, M., Lerch, J.P., Vuust, P., 2015. Gray- and white-matter anatomy of absolute pitch possessors. *Cereb. Cortex* 25, 1379–1388.
- Elmer, S., Rogenmoser, L., Kühnis, J., Jäncke, L., 2015. Bridging the gap between perceptual and cognitive perspectives on absolute pitch. *J. Neurosci.* 35, 366–371.
- Engel, A.K., Fries, P., 2010. Beta-band oscillations—signalling the status quo? *Curr. Opin. Neurobiol.* 20, 156–165.
- Finger, H., Bönstrup, M., Cheng, B., Messé, A., Hilgetag, C., Thomalla, G., Gerloff, C., König, P., 2016. Modeling of large-scale functional brain networks based on structural connectivity from DTI: comparison with EEG derived phase coupling networks and evaluation of alternative methods along the modeling path. *PLoS Comput. Biol.* 12, e1005025.
- Friederici, A.D., 2002. Towards a neural basis of auditory sentence processing. *Trends Cogn. Sci.* 6, 78–84.
- Fuchs, M., Kastner, J., Wagner, M., Hawes, S., Ebersole, J.S., 2002. A standardized boundary element method volume conductor model. *Clin. Neurophysiol.* 113, 702–712.
- Fuster, J.M., 2006. The cognit: a network model of cortical representation. *Int. J. Psychophysiol.* 60, 125–132.
- Gordon, E.E., 1989. *Manual for the Advanced Measures of Music Education*.
- Greber, M., Rogenmoser, L., Elmer, S., Jäncke, L., 2018. Electrophysiological correlates of absolute pitch in a passive auditory oddball paradigm: a direct replication attempt. *eNeuro* 5 (ENEURO-0333).
- Griffiths, T.D., Warren, J.D., 2002. The planum temporale as a computational hub. *Trends Neurosci.* 25, 348–353.
- Halsey, L.G., Curran-Everett, D., Vowler, S.L., Drummond, G.B., 2015. The fickle P value generates irreproducible results. *Nat. Methods* 12, 179–185.
- Hickok, G., Poeppel, D., 2007. The cortical organization of speech processing. *Nat. Rev. Neurosci.* 8, 393–402.
- Hsieh, L.T., Ranganath, C., 2014. Frontal midline theta oscillations during working memory maintenance and episodic encoding and retrieval. *Neuroimage* 85, 721–729.
- Ioannidis, J.P.A., 2008. Why most discovered true associations are inflated. *Epidemiology* 19, 640–648.
- Jäncke, L., Langer, N., 2011. A strong parietal hub in the small-world network of coloured-hearing synaesthetes during resting state EEG. *J. Neuropsychol.* 5, 178–202.
- Jäncke, L., Langer, N., Hänggi, J., 2012. Diminished whole-brain but enhanced perisylvian connectivity in absolute pitch musicians. *J. Cogn. Neurosci.* 24, 1447–1461.
- Jung, T.P., Makeig, S., Humphries, C., Lee, T.W., McKeown, M.J., Iragui, V., Sejnowski, T.J., 2000. Removing electroencephalographic artifacts by blind source separation. *Psychophysiology* 37, 163–178.
- Keenan, J.P., Thangaraj, V., Halpern, A.R., Schlaug, G., 2001. Absolute pitch and planum temporale. *Neuroimage* 14, 1402–1408.
- Kim, S.-G., Knösche, T.R., 2017a. On the perceptual subprocess of absolute pitch. *Front. Neurosci.* 11, 1–6.
- Kim, S.-G., Knösche, T.R., 2017b. Resting state functional connectivity of the ventral auditory pathway in musicians with absolute pitch. *Hum. Brain Mapp.* 38, 3899–3916.

- Klein, C., Liem, F., Hänggi, J., Elmer, S., Jäncke, L., 2015. The “silent” imprint of musical training. *Hum. Brain Mapp.* 37, 536–546.
- Klein, C., Metz, S.I., Elmer, S., Jäncke, L., 2018. The interpreter’s brain during rest—hyperconnectivity in the frontal lobe. *PLoS One* 13, 1–17.
- Lawrence, M.A., 2016. *Ez: Easy Analysis and Visualization of Factorial Experiments*. Cambridge University Press, Cambridge.
- Lehrl, S., 2005. *Manual zum MWT-B*.
- Leipold, S., Brauchli, C., Greber, M., Jäncke, L., 2019a. Absolute and relative pitch processing in the human brain: neural and behavioral evidence. *Brain Struct. Funct.* 224, 1723–1738.
- Leipold, S., Greber, M., Elmer, S., 2019b. Perception and cognition in absolute pitch: distinct yet inseparable. *J. Neurosci.* 39, 5839–5841.
- Leipold, S., Greber, M., Sele, S., Jäncke, L., 2019c. Neural patterns reveal single-trial information on absolute pitch and relative pitch perception. *Neuroimage* 200, 132–141.
- Leipold, S., Oederbolz, C., Greber, M., Jäncke, L., 2019d. A reevaluation of the electrophysiological correlates of absolute pitch and relative pitch: no evidence for an absolute pitch-specific negativity. *Int. J. Psychophysiol.* 137, 21–31.
- Levitin, D.J., 1994. Absolute memory for musical pitch: evidence from the production of learned melodies. *Percept. Psychophys.* 56, 414–423.
- Levitin, D.J., Rogers, S.E., 2005. Absolute pitch: perception, coding, and controversies. *Trends Cogn. Sci.* 9, 26–33.
- Loui, P., Li, H.C., Hohmann, A., Schlaug, G., 2011. Enhanced cortical connectivity in absolute pitch musicians: a model for local hyperconnectivity. *J. Cogn. Neurosci.* 23, 1015–1026.
- Loui, P., Zamm, A., Schlaug, G., 2012. Enhanced functional networks in absolute pitch. *Neuroimage* 63, 632–640.
- Luders, E., Gaser, C., Jäncke, L., Schlaug, G., 2004. A voxel-based approach to gray matter asymmetries. *Neuroimage* 22, 656–664.
- Makris, N., Kennedy, D.N., McInerney, S., Sorensen, A.G., Wang, R., Caviness, V.S., Pandya, D.N., 2005. Segmentation of subcomponents within the superior longitudinal fascicle in humans: a quantitative, in vivo, DT-MRI study. *Cereb. Cortex* 15, 854–869.
- Mazziotta, J., Toga, A., Evans, A., Fox, P., Lancaster, J., Zilles, K., Woods, R., Paus, T., Simpson, G., Pike, B., Holmes, C., Collins, L., Thompson, P., MacDonald, D., Iacoboni, M., Schormann, T., Amunts, K., Palomero-Gallagher, N., Geyer, S., Parsons, L., Narr, K., Kabani, N., Le Goualher, G., Boomsma, D., Cannon, T., Kawashima, R., Mazoyer, B., 2001. A probabilistic atlas and reference system for the human brain: International Consortium for Brain Mapping (ICBM). *Philos. Trans. R. Soc. Lond. Ser. B Biol. Sci.* 356, 1293–1322.
- McKetton, L., DeSimone, K., Schneider, K.A., 2019. Larger auditory cortical area and broader frequency tuning underlie absolute pitch. *J. Neurosci.* 39, 2930–2937.
- Morey, R.D., Rouder, J.N., Jamil, T., 2018. **Computation of Bayes factors for common designs. R package version 0.9.12-4.2 [WWW document].** URL: <https://cran.r-project.org/web/packages/BayesFactor/index.html>.
- Näpflin, M., Wildi, M., Sarnthein, J., 2007. Test-retest reliability of resting EEG spectra validates a statistical signature of persons. *Clin. Neurophysiol.* 118, 2519–2524.
- Nichols, T.E., Holmes, A.P., 2001. Nonparametric permutation tests for functional neuroimaging: a primer with examples. *Hum. Brain Mapp.* 15, 1–25.
- Oechslin, M.S., Imfeld, A., Loenneker, T., Meyer, M., Jäncke, L., 2010a. The plasticity of the superior longitudinal fasciculus as a function of musical expertise: a diffusion tensor imaging study. *Front. Hum. Neurosci.* 3, 76.
- Oechslin, M.S., Meyer, M., Jäncke, L., 2010b. Absolute pitch-functional evidence of speech-relevant auditory acuity. *Cereb. Cortex* 20, 447–455.
- Ohnishi, T., Matsuda, H., Asada, T., Aruga, M., Hirakata, M., Nishikawa, M., Katoh, A., Imabayashi, E., 2001. Functional anatomy of musical perception in musicians. *Cereb. Cortex* 11, 754–760.
- O’Reilly, R.C., 2010. The what and how of prefrontal cortical organization the What-How, Abstraction, Cold/Hot (WHACH) model of PFC organization. *Trends Neurosci.* 33, 355–361.
- O’Reilly, C., Elabbagh, M., 2020. Intracranial Recordings Reveal Ubiquitous in-Phase and in-Antiphase Functional Connectivity between Homologous Brain Regions in Humans. (bioRxiv 2020.06.19.162065).
- Paranjape, R.B., Mahovsky, J., Benedicenti, L., Koles, Z., 2001. The electroencephalogram as a biometric. *Canadian Conference on Electrical and Computer Engineering* 2, 1363–1366.
- Pascual-Marqui, R.D., 2007. Instantaneous and Lagged Measurements of Linear and Nonlinear Dependence between Groups of Multivariate Time Series: Frequency Decomposition. arXiv:0711.1455 [stat.ME] 2007-Noem. pp. 1–18.
- Pascual-Marqui, R.D., Lehmann, D., Koukkou, M., Kochi, K., Anderer, P., Saletu, B., Tanaka, H., Hirata, K., John, E.R., Prichep, L., Biscay-Lirio, R., Kinoshita, T., 2011. Assessing interactions in the brain with exact low-resolution electromagnetic tomography. *Philos. Trans. A Math. Phys. Eng. Sci.* 369, 3768–3784.
- Petersen, S.E., Sporns, O., 2015. Brain networks and cognitive architectures. *Neuron* 88, 207–219.
- Plakke, B., Romanski, L.M., 2014. Auditory connections and functions of prefrontal cortex. *Front. Neurosci.* 8, 1–13.
- Poulos, M., Rangoussi, M., Alexandris, N., Evangelou, A., 2002. Person identification from the EEG using nonlinear signal classification. *Methods Inf. Med.* 41, 64–75.
- R Core Team, 2017. *R: A Language and Environment for Statistical Computing*.
- Rauschecker, J.P., 2011. An expanded role for the dorsal auditory pathway in sensorimotor control and integration. *Hear. Res.* 271, 16–25.
- Rauschecker, J.P., Scott, S.K., 2009. Maps and streams in the auditory cortex: nonhuman primates illuminate human speech processing. *Nat. Neurosci.* 12, 718–724.
- Rouder, J.N., Speckman, P.L., Sun, D., Morey, R.D., Iverson, G., 2009. Bayesian t tests for accepting and rejecting the null hypothesis. *Psychon. Bull. Rev.* 16, 225–237.
- Schlaug, G., Jäncke, L., Huang, Y., Steinmetz, H., 1995. In vivo evidence of structural brain asymmetry in musicians. *Science* 267, 699–701.
- Schulze, K., Gaab, N., Schlaug, G., 2009. Perceiving pitch absolutely: comparing absolute and relative pitch possessors in a pitch memory task. *BMC Neurosci.* 10.
- Siegel, M., Donner, T.H., Engel, A.K., 2012. Spectral fingerprints of large-scale neuronal interactions. *Nat. Rev. Neurosci.* 13, 121–134.
- Sporns, O., Chialvo, D.R., Kaiser, M., Hilgetag, C.C., 2004. Organization, development and function of complex brain networks. *Trends Cogn. Sci.* 8, 418–425.
- Srinivasan, R., Tucker, D.M., Murias, M., 1998. Estimating the spatial Nyquist of the human EEG. *Behav. Res. Methods Instrum. Comput.* 30, 8–19.
- Teffer, K., Semendeferi, K., 2012. *Human Prefrontal Cortex. Evolution, Development, and Pathology*, 1st ed. Elsevier B.V.
- Valizadeh, S.A., Riener, R., Elmer, S., Jäncke, L., 2019. Decrypting the electrophysiological individuality of the human brain: identification of individuals based on resting-state EEG activity. *Neuroimage* 197, 470–481.
- Wang, X.J., 2010. Neurophysiological and computational principles of cortical rhythms in cognition. *Physiol. Rev.* 90, 1195–1268.
- Ward, L.M., 2003. Synchronous neural oscillations and cognitive processes. *Trends Cogn. Sci.* 7, 553–559.
- Wengenroth, M., Blatow, M., Heinecke, A., Reinhardt, J., Stippich, C., Hofmann, E., Schneider, P., 2014. Increased volume and function of right auditory cortex as a marker for absolute pitch. *Cereb. Cortex* 24, 1127–1137.
- Wenhardt, T., Bethlehem, R.A.L., Baron-Cohen, S., Altenmüller, E., 2019. Autistic traits, resting-state connectivity, and absolute pitch in professional musicians: shared and distinct neural features. *Mol. Autism* 10, 1–18.
- Wilson, S.J., Lusher, D., Wan, C.Y., Dudgeon, P., Reutens, D.C., 2009. The neurocognitive components of pitch processing: insights from absolute pitch. *Cereb. Cortex* 19, 724–732.
- Xu, J., Wang, J., Fan, L., Li, H., Zhang, W., Hu, Q., Jiang, T., 2015. Tractography-based parcellation of the human middle temporal gyrus. *Sci. Rep.* 5, 1–13.
- Zalesky, A., Fornito, A., Bullmore, E.T., 2010. Network-based statistic: identifying differences in brain networks. *Neuroimage* 53, 1197–1207.
- Zatorre, R.J., Perry, D.W., Beckett, C.A., Westbury, C.F., Evans, A.C., 1998. Functional anatomy of musical processing in listeners with absolute pitch and relative pitch. *Proc. Natl. Acad. Sci. U. S. A.* 95, 3172–3177.
- Zumsteg, D., Friedman, A., Wennberg, R.A., Wieser, H.G., 2005. Source localization of mesial temporal interictal epileptiform discharges: correlation with intracranial foramen ovale electrode recordings. *Clin. Neurophysiol.* 116, 2810–2818.
- Zumsteg, D., Lozano, A.M., Wennberg, R.A., 2006. Depth electrode recorded cerebral responses with deep brain stimulation of the anterior thalamus for epilepsy. *Clin. Neurophysiol.* 117, 1602–1609.